

## Supporting Information for:

# Gas-Phase Formation of Glycolonitrile in the Interstellar Medium

Luis Guerrero-Méndez,<sup>a</sup> Anxo Lema-Saavedra,<sup>b</sup> Elena Jiménez,<sup>c,d</sup> Antonio Fernández-Ramos,<sup>\*a,b</sup> and Emilio Martínez-Núñez<sup>\*a</sup>

<sup>a</sup>Departamento de Química Física, Facultade de Química, Universidade de Santiago de Compostela, Avda. das Ciencias s/n 15782, Santiago de Compostela, Spain. E-mail: [gf.ramos@usc.es](mailto:gf.ramos@usc.es), [emilio.nunez@usc.es](mailto:emilio.nunez@usc.es)

<sup>b</sup>Centro Singular de Investigación en Química Biológica y Materiales Moleculares (CIQUS), Universidade de Santiago de Compostela, C/Jenaro de la Fuente s/n, 15782, Santiago de Compostela, Spain

<sup>c</sup>Departamento de Química Física, Facultad de Ciencias y Tecnologías Químicas, Universidad de Castilla-La Mancha, Avda. Camilo José Cela 1b, 13071, Ciudad Real, Spain

<sup>d</sup>Instituto de Investigación en Combustión y Contaminación Atmosférica (ICCA), Universidad de Castilla-La Mancha, Camino de Moledores s/n, 13071, Ciudad Real, Spain

<b>Fig. S1</b> Product abundances as a function of number of iterations.....	S3
<b>Fig. S2</b> Additional CN+ CH <sub>2</sub> OH pathways .....	S4
<b>Fig. S3</b> Additional OH + CH <sub>2</sub> NC pathway.....	S5
<b>Fig. S4</b> Additional 3-step HCO + CH <sub>2</sub> N pathways.....	S6
<b>Fig. S5</b> Additional longer HCO + CH <sub>2</sub> N pathways.....	S7
<b>Fig. S6</b> Additional radical-molecule pathway.....	S8
<b>Table S1</b>	
Rate coefficients for the OH+CH <sub>2</sub> CN→HNC+CH <sub>2</sub> O reaction .....	S9
<b>Table S2</b>	
Rate coefficients for the OH+CH <sub>2</sub> CNH→GLN+H reaction .....	S9

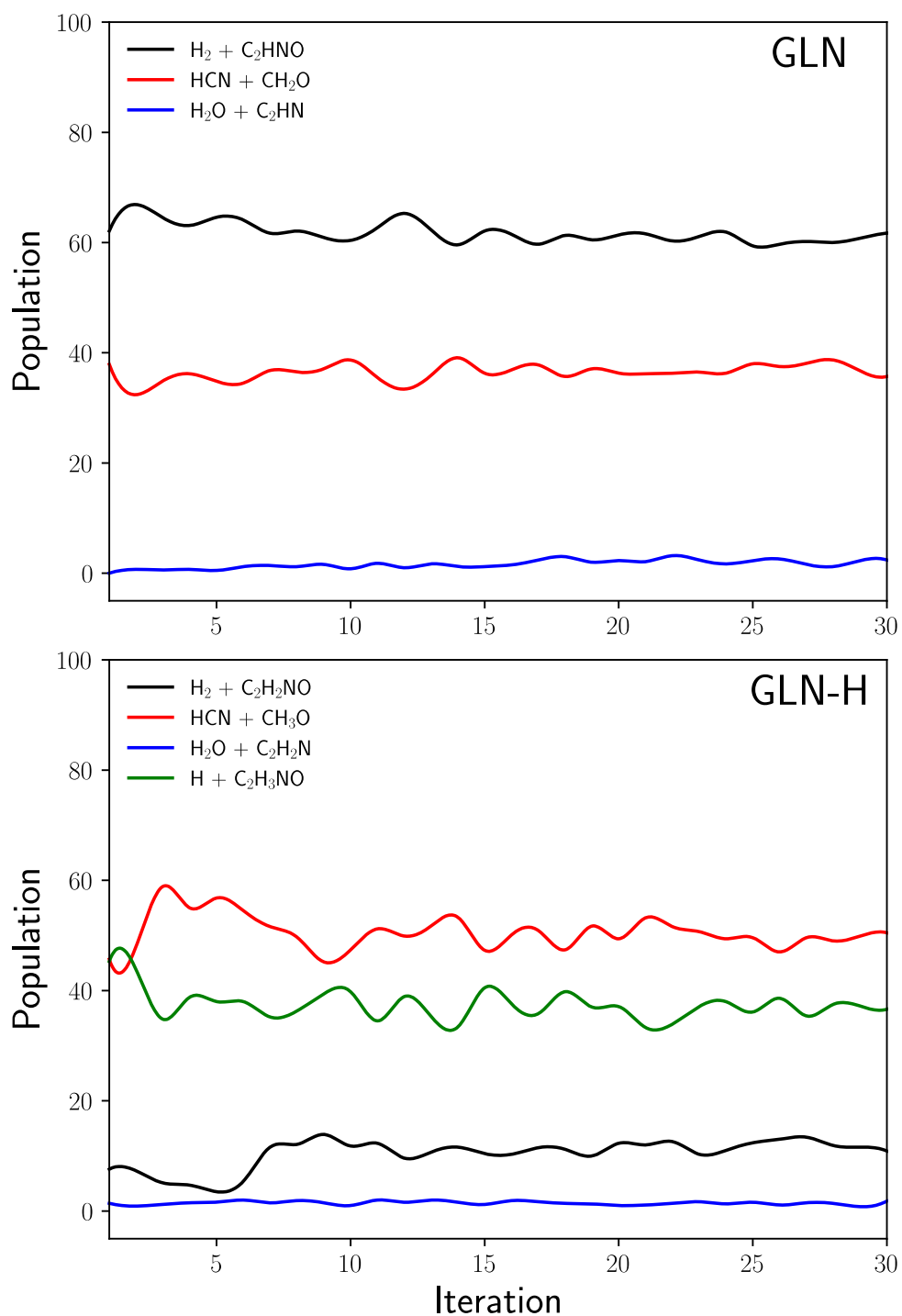


**Fig. S1** Product abundances as a function of number of iterations obtained from the KMC simulations for GLN and GLN-H, using an excitation energy of 250 kcal/mol. The Level1-calculated energies and vibrational frequencies are employed in the calculations of the RRKM rate coefficients, and barrierless reactions are not included.

The relative energies depicted in Figures S2-S6 are referenced to the initial geometry utilized for the AutoMeKin calculations of the GLN and GLN-H systems.

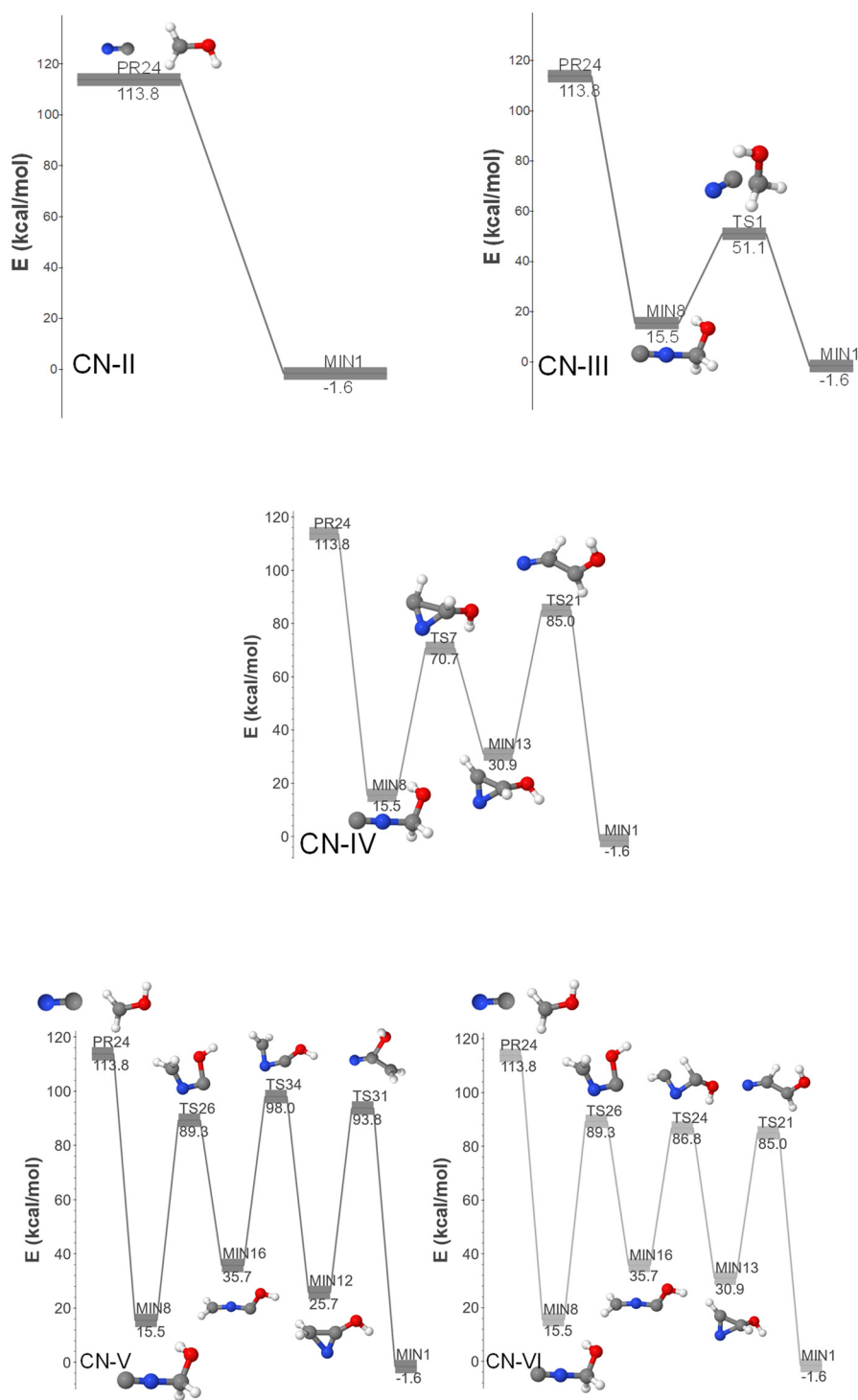


**Fig. S2** Additional DFT-computed energy profiles for the barrierless formation of GLN from CN+CH<sub>2</sub>OH.

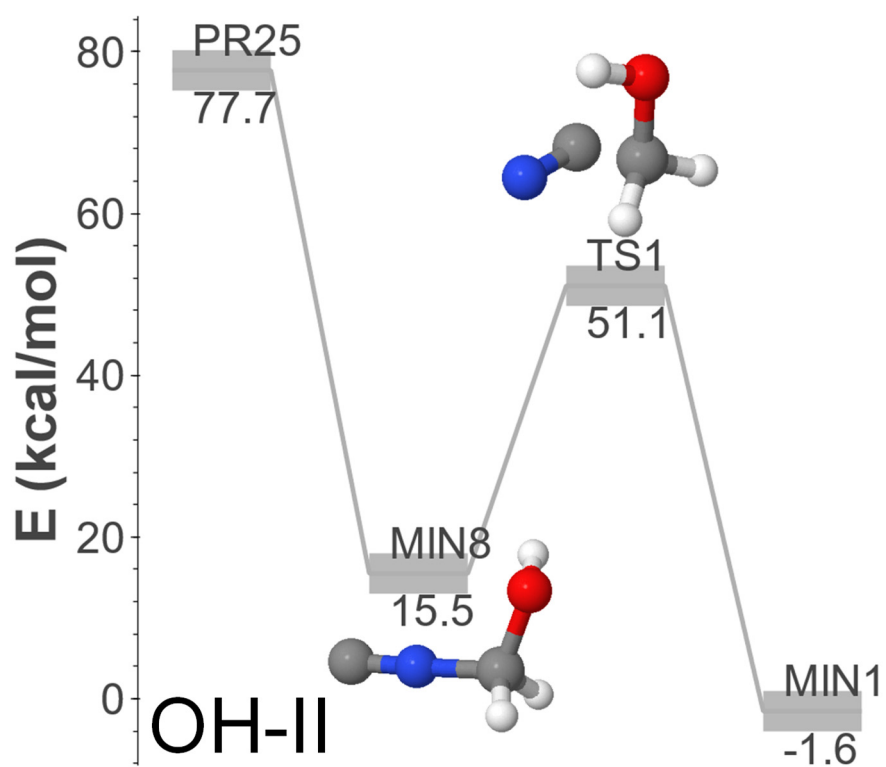


**Fig. S3** Additional DFT-computed energy profile for the barrierless formation of GLN from OH + CH<sub>2</sub>NC (OH-II pathway).

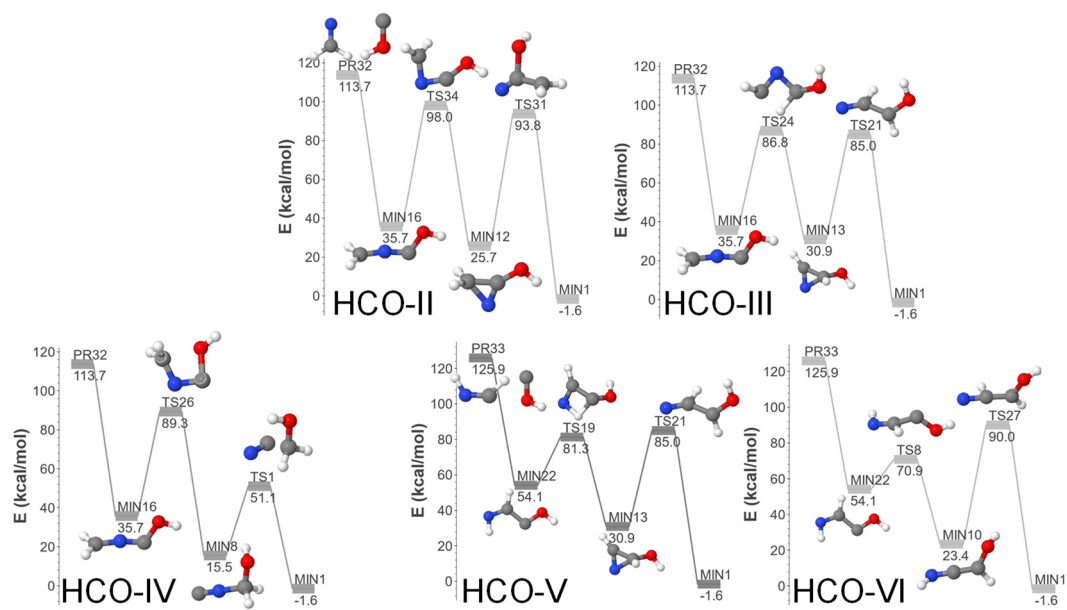


**Fig. S4** Additional DFT-computed energy profiles for the barrierless formation of GLN from HCO + CH<sub>2</sub>N. Pathways involving 3 elementary steps are displayed.

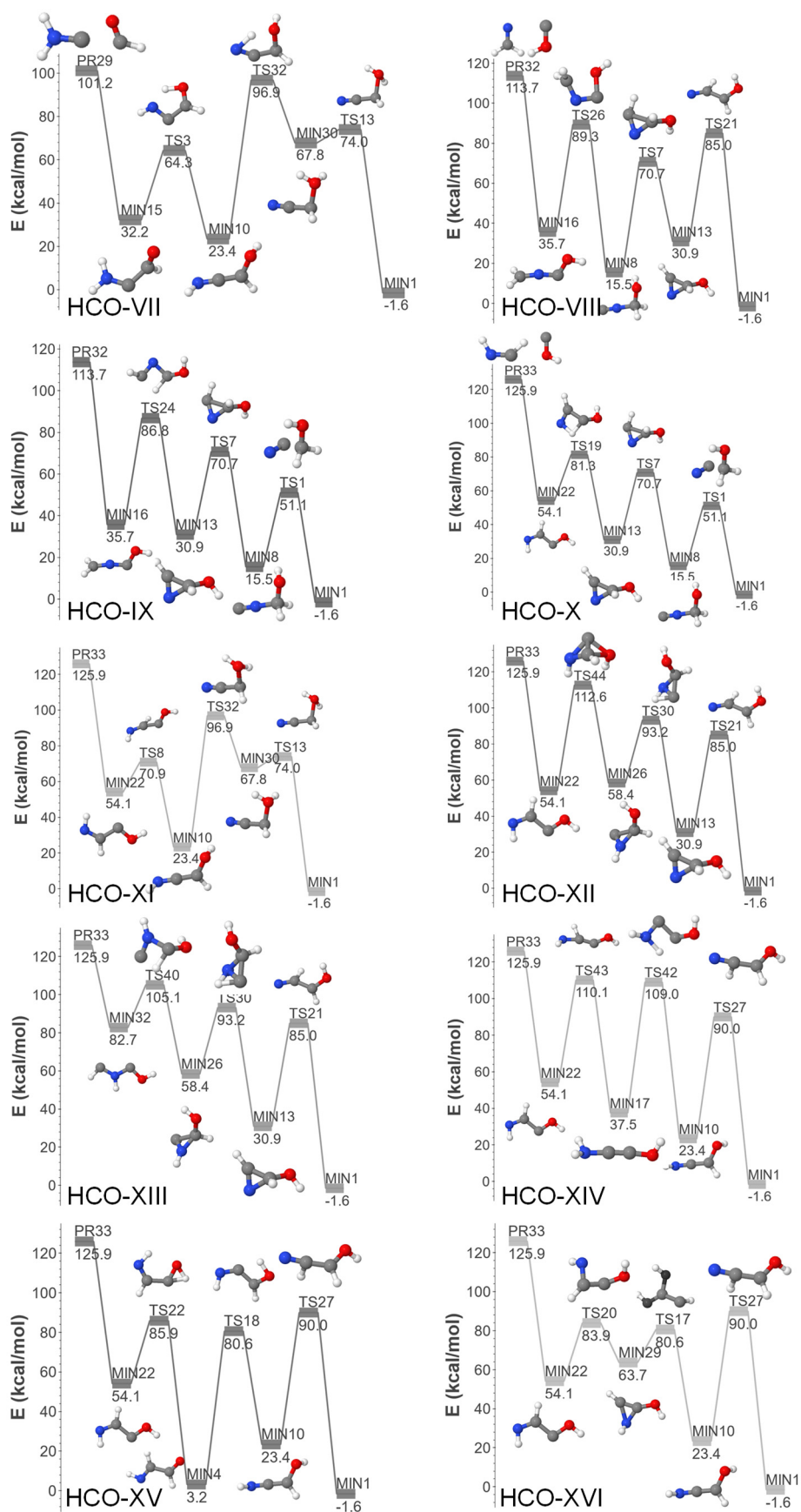


**Fig. S5** Additional DFT-computed energy profiles for the barrierless formation of GLN from HCO + CH<sub>2</sub>N. Pathways involving 4 elementary steps are displayed.

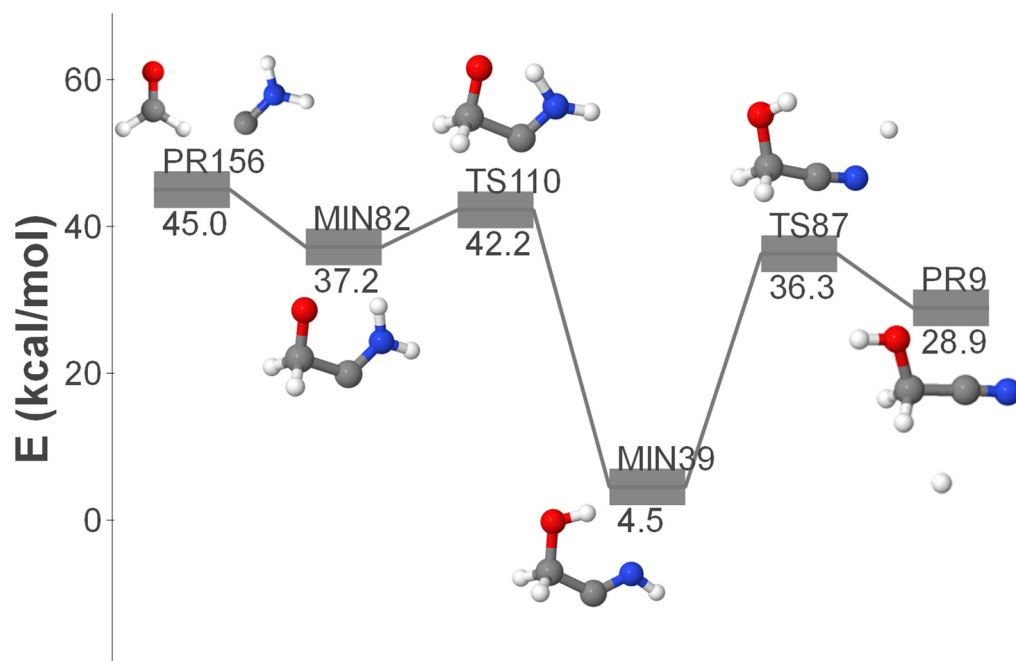


**Fig. S6** Additional DFT-computed energy profile for the barrierless (radical-molecule) formation of GLN+H.



**Table S1:** Rate coefficients (in  $\text{cm}^3 \text{ molecule}^{-1} \text{ s}^{-1}$ ) for the  $\text{OH}+\text{CH}_2\text{CN}\rightarrow\text{HNC}+\text{CH}_2\text{O}$  reaction

$T/\text{K}$	$k_1$	$k_2$	$k^{\text{CUS}}$
10	1.15E-09	2.90E+243	1.15E-09
20	1.02E-09	5.57E+115	1.02E-09
30	9.55E-10	1.15E+73	9.55E-10
40	9.11E-10	4.60E+51	9.11E-10
50	8.78E-10	6.19E+38	8.78E-10
60	8.51E-10	1.56E+30	8.51E-10
70	8.30E-10	1.09E+24	8.30E-10
80	8.11E-10	2.58E+19	8.11E-10
90	7.96E-10	6.45E+15	7.96E-10
100	7.82E-10	8.39E+12	7.82E-10
110	7.69E-10	3.64E+10	7.69E-10
120	7.58E-10	3.89E+08	7.58E-10
130	7.48E-10	8.34E+06	7.48E-10
140	7.39E-10	3.09E+05	7.39E-10
150	7.31E-10	1.77E+04	7.31E-10

**Table S2:** Rate coefficients (in  $\text{cm}^3 \text{ molecule}^{-1} \text{ s}^{-1}$ ) for the  $\text{OH}+\text{CH}_2\text{CNH}\rightarrow\text{GLN}+\text{H}$  reaction

$T/\text{K}$	$k_1$	$k_2$	$k^{\text{CUS}}$
10	6.61E-10	5.79E+16	6.61E-10
20	5.89E-10	3.16E+02	5.89E-10
30	5.51E-10	4.29E-03	5.51E-10
40	5.25E-10	1.40E-05	5.25E-10
50	5.06E-10	4.26E-07	5.05E-10
60	4.91E-10	4.01E-08	4.85E-10
70	4.78E-10	7.31E-09	4.49E-10
80	4.68E-10	2.02E-09	3.80E-10
90	4.59E-10	7.41E-10	2.83E-10
100	4.51E-10	3.32E-10	1.91E-10
110	4.43E-10	1.73E-10	1.24E-10
120	4.37E-10	1.00E-10	8.15E-11
130	4.31E-10	6.35E-11	5.53E-11
140	4.26E-10	4.30E-11	3.91E-11
150	4.21E-10	3.09E-11	2.88E-11